

# Analysis and Modeling of State-Dependent Delay in Control Valves

Mads Valentin Bram\* Jan-Peter Calliess\*\*  
 Stephen Roberts\*\* Dennis Severin Hansen\* Zhenyu Yang\*

\* Department of Energy Technology, Aalborg University, Esbjerg  
 Campus, Niels Bohrs Vej 8, 6700 Esbjerg, Denmark (e-mail:  
 mvb@et.aau.dk, dsh@et.aau.dk, yang@et.aau.dk).

\*\* Department of Engineering, Oxford University, Oxford-Man  
 Institute of Quantitative Finance, Eagle House, Walton Well Road,  
 Oxford, OX2 6ED, United Kingdom (e-mail:  
 jan-peter.calliess@oxford-man.ox.ac.uk, sjrob@robots.ox.ac.uk).

**Abstract:** Pneumatic control valves are deployed in a wide variety of industrial applications and plants. The plethora of valve applications has a great span in required operational accuracy and time scales, from precise medical dosing valves to large valves used for level control in offshore separation tanks. It is common for these valves to have inherent position control deployed by the manufacturer, and as a result, these valve systems often receive a wanted opening degree, where the inherent position control drives the actual valve opening towards the wanted opening degree. From previous works utilizing pneumatic control valves for offshore produced water treatment, an inconsistent input-output delay was observed. This work presents experiments to detect and describe these delays, such that the model may be incorporated in the design of improved control solutions that account for these behaviors. A pin-cart model with state-dependent delay is proposed, validated using data from a continuously actuated valve, and compared to commonly used existing valve models. The proposed model exerts the state-dependent input-output delay successfully.

*Keywords:* Process modeling, Valve system, Time delay, Backlash, Hybrid system.

## 1. INTRODUCTION

Control valves are ubiquitous in various industrial process plants; from the food industry to the offshore oil and gas sector. An industrial study by Desborough and Miller (2002) estimates that control valve problems account for 32% of controllers being classified as having "poor" or "fair" performance, which results in large economic losses. Improving process control often yields direct economic benefit, especially in those industries where control valves are abundant, such as the offshore oil & gas industry. In the offshore oil & gas industry, many multi-phase separation technologies that utilize control valves are deployed. Some of these separation technologies include enhanced gravimetric separation by hydrocyclones and membrane filtration systems (Jepsen et al. (2018)). A common trait of liquid-liquid hydrocyclones and membrane filtration systems is the relatively high speed of their hydrodynamic interactions between pressure and flow rate compared to the relatively slow speed of the valves assigned to control them. Noteworthy are the exceptions of various types of wear and fouling, which can be much slower than the valves (Jepsen et al. (2018)).

As these valves' dynamics have a dominant influence on the process's dynamic response, there is a strong incentive to account for the nonlinear valve behaviors in the control solution (Jepsen et al. (2018); Jelali (2006)). The most commonly observed nonlinearities of valve systems include

slew rate, dead-time, hysteresis, stiction, backlash, and deadband (Choudhury et al. (2004, 2005); Jelali (2006)).

Control valves are typically configured in closed loop as shown in Fig. 1. The reference set-point ( $S_P$ ) is provided by a human operator or higher-level control loops, the process controller ( $C_{process}$ ) aims to reduce the error between  $S_P$  and the process variable ( $P_V$ ), the output of  $C_{process}$  is the wanted valve position ( $O_P$ ), the output ( $O_V$ ) of the valve position controller ( $C_{valve}$ ) aims to reduce the position error between the actual valve position ( $V_P$ ) and  $O_P$ , and the often nonlinear interaction between  $V_P$  and the manipulated variable ( $M_V$ ) is described by the valve's opening characteristics ( $V_{fluid}$ ), which also affects  $P_V$  depending on the plant (Shoukat Choudhury et al. (2005); Bacci di Capaci and Scali (2018)).

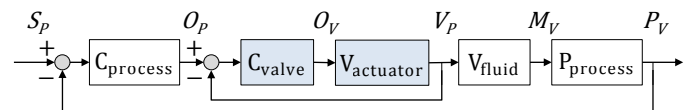


Fig. 1. A common control valve structure system structure, where the inner loop is valve position control (blue) and the outer loop is plant process control

Several studies and previous works have investigated the modeling of the closed loop dynamic and static relationship between  $O_P$  and  $V_P$ , or  $O_P$  and  $M_V$  of various control solutions (Bacci di Capaci and Scali (2018); Bram et al.

(2015)). These models are significantly dependent on the valve type and properties as well as the type of inner loop control. Large differences in process sensitivity are addressed via a large variety of valve models; from simple first-order transfer functions to intrinsic nonlinear models (Bacci di Capaci and Scali (2018); Bram et al. (2015)). Preliminary analysis can be used as decision support for a convenient choice of valve model. Noteworthy control valve analysis procedures, that require either dedicated experiments (invasive) or available data (non-invasive), have been summarized in (Choudhury et al. (2005)). As a general modeling practice, the tradeoff between model simplicity and correctness must be balanced in accordance with the purpose and requirements of the plant. Medical dosing is an example of requiring high accuracy and precision, as small errors may have large consequences, whereas general water level control is more forgiving as long as the level is maintained within some upper and lower safety level (Durdevic and Yang (2018); Hansen et al. (2018b)). First-principle models are not feasible in all applications as they require several physical parameters that might not be known, such as spring constant, air pressure, and mass (Bacci di Capaci and Scali (2018)). Additionally, the computation time can be excessively high due to numerical integrations (He and Wang (2014)). Grey- and black-box models can be utilized if physical parameters are unknown, such as first-order-plus-dead-time (FOPDT) models or the stiction model proposed by Shoukat Choudhury et al. (2005). The main observed drawback of the FOPDT models is the fixed time delay that might not be a sufficient simplification of the apparent backlash of the system. The stiction model excels at emulating "stick-slip" behavior of valves, but might not be as well suited for transient dynamical behaviors. This paper investigates the modeling and validation of the inner control loop of a valve system as observed externally as a closed loop. As such, the proposed model is designed to support better adaptive control solutions in process plants where relatively high accuracy and precision of valve actuation are demanded. Specifically, this work's contributions are:

- (1) Analysis of deadband behavior that in closed loop is experienced as a state-dependent delay.
- (2) A proposed pin-cart modeling approach for describing this state-dependent delay.
- (3) Validation of the proposed model and comparison with other commonly used valve models.

The rest of the paper is organized as follows: Section 2 describes the proposed pin-cart model, Section 3 describes the used materials and execution of the experiments, Section 4 shows the experiment results, Section 5 discusses the validation of the proposed model, and Section 6 provides concluding remarks.

## 2. PIN-CART MODEL

This section will propose a model structure with parameters that quantify specific input-output behaviors. This approach is chosen to avoid requiring all the physical specifications of the valve and instead identify the parameters experimentally. Additionally, while it is possible to define the structure of a physics-based model from first principles, it requires more parameters, some with

unknown influence, related to the input-output relationship. Furthermore, the model is defined so that it is easily implementable into the other process models, such as the grey-box hydrocyclone model described in Bram et al. (2017, 2018, 2019). The pin-cart model will be part of a larger framework that facilitates better adaptive control solutions for deoiling applications. From the observation of the experiment described in Section 3.1, the proposed model structure is heavily inspired by how a cart, free to move in one dimension, can be pushed by a controlled pin that is always bounded by the sides of the cart as seen in Fig. 2. The combination of the continuous movement and discrete engage events classify the pin-cart model as a hybrid system (Antsaklis (2000)).

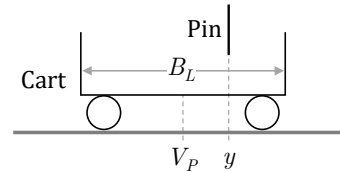


Fig. 2. Schematic analogy of the pin-cart model with the cart's position  $V_P$  and the pin's position  $y$  along the horizontal axis

### 2.1 Pin-Cart Model Structure

The following equations will describe the execution of the pin-cart model that predicts  $V_P$  at the next time step. The inner loop valve position error ( $e$ ) at time step ( $k$ ) is

$$e(k) = O_P(k) - V_P(k). \quad (1)$$

As the output of the inner loop controller relates to the pin speed, a P controller is used to emulate the pin speed, by updating the pin position ( $y(k)$ ) as

$$y(k+1) = y(k) + P_k \cdot e(k), \quad (2)$$

where  $P_k$  is the controller's proportional gain. Normally, the actual implemented  $C_{valve}$  is a PI or PID controller to eliminate steady state error and reduce settling time and overshoot. However, these controller types were found to yield insignificant increased model prediction performance when used in (2), thus a P controller was selected.  $V_P$  is lastly updated as

$$V_P(k+1) = \begin{cases} y(k+1) - \frac{B_L}{2}, & \text{if } y(k+1) - V_P(k) \geq \frac{B_L}{2} \\ y(k+1) + \frac{B_L}{2}, & \text{if } y(k+1) - V_P(k) \leq -\frac{B_L}{2} \\ V_P(k), & \text{otherwise} \end{cases} \quad (3)$$

where  $B_L$  is a constant relating to the magnitude of apparent backlash and  $V_P(k)$  is the model output. The term  $\frac{B_L}{2}$  is used to assign  $V_P$  to the center of the cart. Equation (3) formulates that the cart stands still when the pin travels between the cart's two sides until the pin engages with either one of the sides. This behavior results in delayed output when the cart changes direction. The length of this delay can be tuned by choosing  $B_L$ , as this is the traveling length of the pin. This model structure has two parameters  $P_k$  and  $B_L$  and is referred to as pin-cart I.

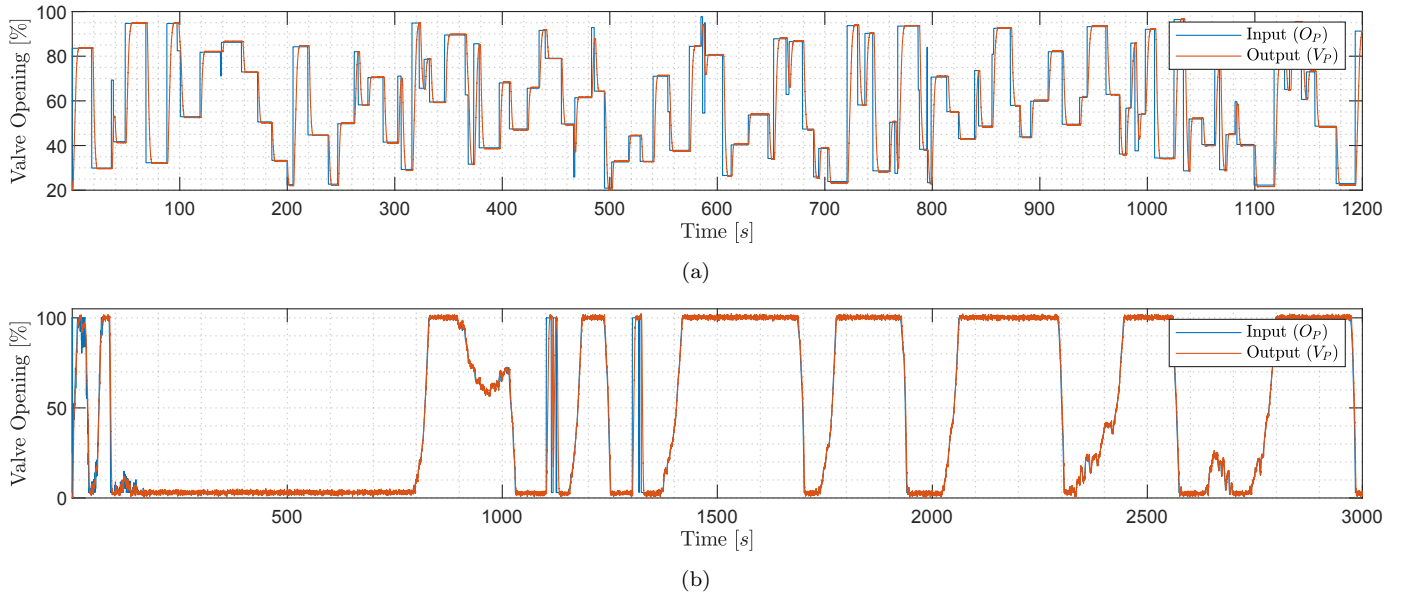


Fig. 3. Input ( $O_P$ ) and output ( $V_P$ ), of the closed loop valve system during the experiments: (a) shows the random stepping experiment and (b) shows the controlled normal operation experiment

## 2.2 Extension of Pin-Cart Model

Additional input-output behaviors can be accounted for by modifying or extending (2). This work includes maximum travel speed, also called slew rate, ( $\Delta y_{max}$ ) as well as minimum non-zero constant pin speed ( $\Delta y_{min}$ ). Minimum non-zero constant pin speed is implemented as

$$\Delta y^*(k) = \text{sgn}(e) \cdot \max(|P_k \cdot e|, \Delta y_{min}), \quad (4)$$

where  $\Delta y^*$  is the unsaturated pin speed. The speed is saturated as

$$\Delta y(k) = \begin{cases} \Delta y_{max}, & \text{if } y^*(k) \geq \Delta y_{max} \\ -\Delta y_{max}, & \text{if } y^*(k) \leq -\Delta y_{max} \\ \Delta y^*(k), & \text{otherwise} \end{cases} \quad (5)$$

The pin position is updated as

$$y(k+1) = y(k) + \Delta y(k). \quad (6)$$

## 3. EXPERIMENT DESIGN

This section describes the setup and execution of the experiments. Each experiment gathered input-output data of a Bürkert pneumatic control valve system 8802 that has an inherent internal position controller (Bürkert Fluid Control Systems (2019)). The used valve is installed in a liquid-liquid hydrocyclone setup, which is a part of a scaled offshore pilot plant at Aalborg University in Esbjerg. The further description of the pilot plant can be found in Durdevic et al. (2018); Hansen et al. (2018a). Using Matlab Simulink the input ( $O_P$ ) and output ( $V_P$ ), of the closed loop valve system, are recorded at  $100\text{Hz}$ . The first experiment consists of a series of random steps, to isolate and analyze the input-output delay. The second experiment consists of continuous operation, as an example of normal operation, to validate and benchmark various valve models.

### 3.1 Delay Investigation Experiment

A 20 minutes pseudo-random input signal ( $O_P$ ) between 20% and 97% opening degree, with a uniform-random hold

time between 0s and 20s, is given as input to the valve system. This will excite the valve system to both positive and negative steps with various sizes.

### 3.2 Normal Operation of Control Valve

The experiment used for the normal operation of the control valve was executed and explained in Durdevic and Yang (2018). The controllers used in this experiment were designed to maintain a water level in a tank while also maintaining a pressure difference ratio in a downstream deoiling hydrocyclone, by actuating two valves. While the control objectives are not important for this work, the controlled operation continuously actuate the valves which gives a well representative and generic example of control valves in normal operation.

## 4. RESULTS

This section starts by analyzing the step responses while focusing on the delay and ends by comparing the performance of promising model candidates. The input-output data from both the random experiment and the controlled normal operation are shown in Fig. 3.

### 4.1 Delay Investigation

As the inner control loop minimizes the valve position error, there is little to no offset observed in Fig. 3. Fig. 3 also shows the transient movement of the valve position. A relevant period of time during the random stepping experiment is shown in Fig. 4 that emphasizes specific input-output behaviors. In Fig. 4 it is observed how  $O_P$  drops from 82% to 71% at 138s and then increases to 86% at 139s. In the short period after 138s, there is no decreasing opening of the actual position of the valve before it approaches 86% opening degree, which indicates that the system has a deadband. Fig. 4 also shows how the delay is correlated with valve direction change, such that

when the valve piston changes direction, a longer delay is experienced. From inspecting Fig. 3 and Fig. 4 it is

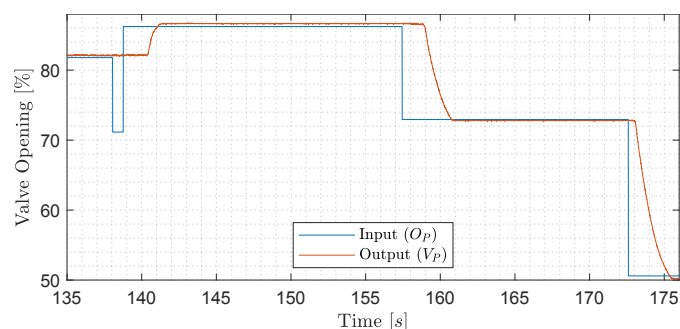


Fig. 4. A segment from the stepping experiment shown in Fig. 3, in the time frame of 135s to 176s, that displays an indication of deadband around 138s, "long" delay around 158s, and "short" delay around 173s

expected that the input-output delay depends on whether  $V_P$  changes or maintains the direction from it's previous step. This delay is shown more clearly in Fig. 5 where all steps are shifted to be concurrent and offset to start from 0%. The blue and red responses indicate whether the valve was in the previous step opened or closed, respectively. It is clear that the shortest delay of  $\approx 0.45$ s is experienced when continuing in the same direction. When changing direction the delay is  $\approx 1$ s, with substantial variation compared to the short delay.

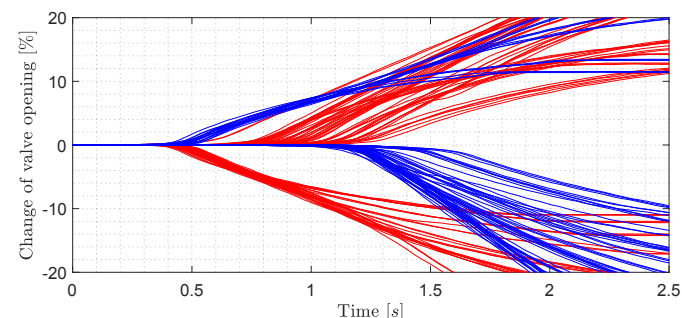


Fig. 5. Collection of all step responses, with the initial opening subtracted for the purpose of illustration. Blue lines indicate that the valve opened previously to achieve initial opening and red lines indicate that the valve closed previously to achieve the initial opening

By acknowledging this behavior and assuming the valve behaves symmetrically, Fig. 6 is generated by inverting the red responses from Fig. 5, such that increasing responses indicate the same direction and decreasing responses indicate a change of direction. Interestingly, the short delays are similar and with smaller variance when compared to the long delay. The responses in Fig. 6 have been colored to indicate the initial opening degree of the individual steps, where blue is near closed, and yellow is near opened. Fig. 6 also shows a tendency that responses that change direction (Negative) have a shorter delay when the initial opening of the response is near closed (blue). The delay of each step from Fig. 6 is shown in Fig. 7 plotted against initial opening. The delay of maintaining direction (black and magenta) is  $\approx 0.45$ s, whereas the delay of changing direction (blue and red) is correlated with the initial

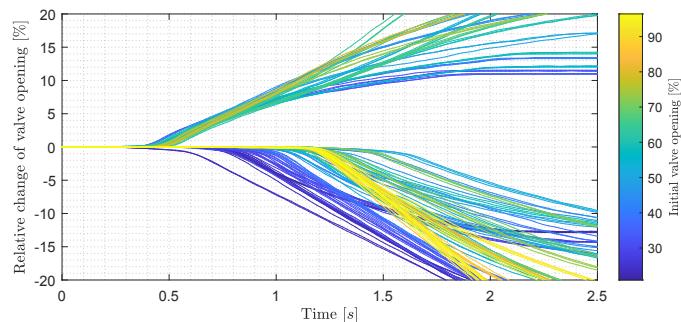


Fig. 6. Increasing step responses are step responses in the same direction as its previous step. Decreasing step responses are step responses with a different direction than its previous step. The color indicates the initial opening of the individual response, where blue is nearly closed and yellow is nearly opened. The delay is significantly lower when the valve has to travel in the same direction as it previously did

opening. The apparent left/right separation of blue and red responses can be attributed to the prior condition, i.e. if the prior step was closing, the initial value of the current step is on average lower, than if the prior step was increasing. The horizontal dashed line is the average delay of maintaining direction and the curved dashed line is the least squares regression fit of a second-order polynomial to the delay of changing direction. To account for this initial

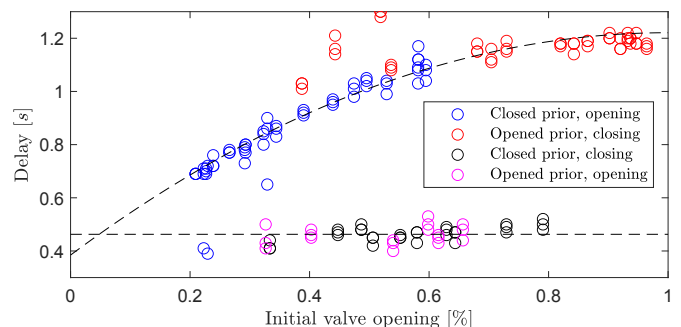


Fig. 7. Shows delay versus absolute initial opening from all step responses. Intuitively, this would relate to piston chamber volume specifically how the volume depends on piston position

position dependent delay, the pin speed can be governed by a function while not engaged with the bounds of the cart:

$$\Delta y(k) = \text{sgn}(e) \cdot (a_p V_P(k)^2 + b_p V_P(k) + c_p)^{-1}, \quad (7)$$

where  $a_p$ ,  $b_p$ , and  $c_p$  are coefficients for the second-order polynomial of the initial position dependent delay also shown in Fig. 7.

#### 4.2 Model Performances and Comparisons

The comparisons in this section include a FOPDT model, a data-driven stiction model as formulated by Shoukat Choudhury et al. (2005) with dead-time, and the two proposed pin-cart models with dead-time. The pin-cart model II includes the state-dependent delay from (7). The FOPDT model has been identified using least square error regression. Both the pin-cart and the stiction models

have parameters that are easily observed and identified from input-output data, which enables them to be tuned conveniently and manually, except for the parameters in (7) which require additional preparation of the data as done in Section 4.1. The pin-cart models behave as intended when  $O_P$  is stepping, as seen in Fig. 8. However, the simple structure from (2) limits the travel of the pin-cart model I to be a first-order step response.

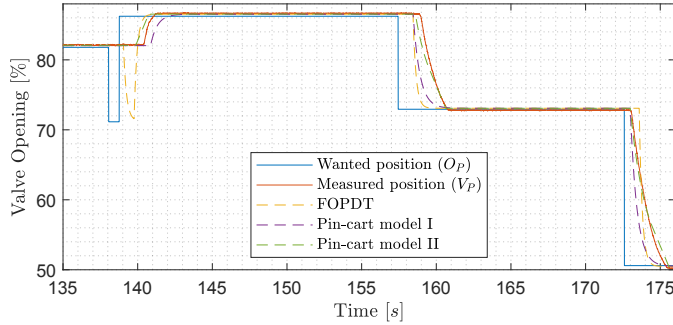


Fig. 8. Model outputs during random stepping. Noteworthy is how the models behave during fast changes around 139s

As the delay is a result of the pin traveling between the cart's two sides, the pin can change direction while traveling, resulting in zero cart movement until the pin engages with either cart side, as seen at around 139s in Fig. 8. This behavior can not be expressed by a FOPDT model, not even if the FOPDT model could switch between two delay values.

During the normal operation experiment  $V_P$  was often saturated at either fully open or fully closed. As a result, the actual pressure difference ratio,  $P_V$ , diverged from the set-point,  $S_P$ , during these time periods. The time periods of interest are those where the outer loop control was able to achieve the control objective by actively manipulating  $O_P$ . Fig. 9 and Fig. 10 show the performance of the models during continuous adjustments of  $O_P$ . The difference in

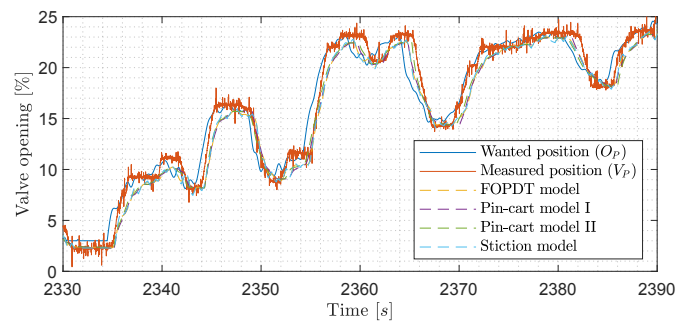


Fig. 9. Model performance during continuous changes of  $O_P$  around 15% opening

the performance of the pin-cart model I between Fig. 9 and Fig. 10 shows the disadvantage of having a fixed  $B_L$  that does not change dependent on initial opening. The pin-cart model II performs significantly better than the FOPDT and the stiction model during the experiment as shown in Fig. 10. The models' performances are summarized in table 1 that lists: mean absolute prediction error of the valve position (MAE), mean absolute prediction error with filtered measured position (MAE filtered), coefficient of

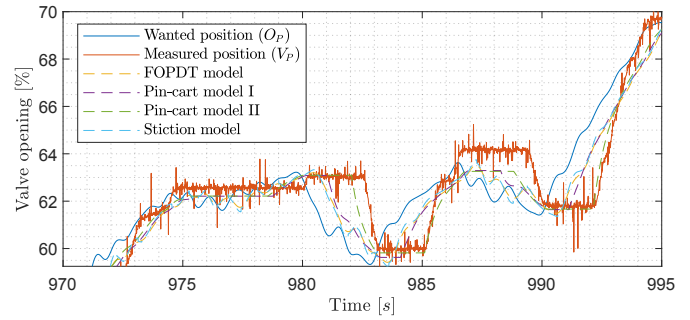


Fig. 10. Model performance during continuous changes of  $O_P$  around 63% opening

determination ( $R^2$ ), sum of squared error (SSE), and sum of squared error relative to having no model (Rel. SSE). The performance metrics are generated from three selected time windows where the valve is not saturated with a total of 413s of data or 41,300 data points. MAE filtered uses a zero-phase 5th order Butterworth filter with a half-power frequency of 1.25Hz for noise reduction on the measured position.

Table 1. Model performance

Model	MAE	MAE filtered	$R^2$	SSE	Rel. SSE
Modelless*	1.106%	1.084%	99.62%	14.37	100 %
Delayed Modelless*	0.876%	0.858%	99.84%	5.917	41.15%
FOPDT	0.869%	0.852%	99.85%	5.770	40.15%
Stiction	0.881%	0.864%	99.84%	5.914	41.15%
Pin-cart I	0.843%	0.825%	99.86%	5.483	38.16%
Pin-cart II	0.731%	0.711%	99.89%	4.284	29.80%

\* This model is a gain of 1, using the input as an estimation of the output.

## 5. DISCUSSION

Even though it is clear that the pin-cart model II performs best, it should be taken into account that it has seven free parameters, whereas the FOPDT model and stiction model only have two and three, respectively, as listed in table 2. The small variance of the short delay observed

Table 2. Summary of model parameters

Model	Free parameters	Count
FOPDT*	Time constant, Time delay ( $T_d$ )	2
Stiction	Stickband, Jumpband, $T_d$	3
Pin-cart I	$B_L, P_k, T_d$	3
Pin-cart II**	$P_k, \Delta y_{max}, \Delta y_{min}, a_p, b_p, c_p, T_d$	7

\* DC Gain is 1 and not a free parameter.

\*\*  $B_L$  is 1 as it is redundant by (7) and not free for this model.

in Fig. 6 is considered attributed to the physical system's response, and not due to the backlash. The large variance of the long delay is attributed to pin travel time plus the physical system's response time, and makes this variance a result of combined uncertainties. The delay being dependent on the initial position, as seen in Fig. 7, is considered attributed to the physical configuration of the valve piston and chamber, specifically the orientation of spring load and air feed. It should not be a question whether or not the mechanical closed loop system has backlash, but rather a question of how significant backlash is (Papageorgiou et al. (2019)). If the backlash is insignificant, then including backlash in the model would yield insignificant

performance improvement at the cost of increased model complexity.

## 6. CONCLUSION

As valves are mechanical systems in the real world, they commonly have undesired intrinsic mechanical properties such as mechanical looseness. These properties are highly valve system dependent and can range from dominant to insignificant behaviors that can be ignored. This paper investigated the input-output relationship of a pneumatic control valve as a closed loop system, from which an intuitive model structure is proposed with coefficients that directly link to observable physical behaviors, such as maximum valve speed and apparent size of backlash. The proposed pin-cart models performed as intended since they can simulate the increased delay when the valve changes direction. This model can be included in larger process models to develop or improve control solutions that demand higher accuracy and precision. The pin-cart behavior is most likely not uniquely intrinsic to valves. In an abstract view, the model can describe a reluctance or delay to change opinion or state. It would be interesting to investigate how this behavior can be implemented in more generalized methods such as neural networks.

## ACKNOWLEDGEMENTS

The authors thank the support from the DTU-DHRTC and AAU joint project - Grey-Box Modeling and Plant-wide Control (AAU Pr-no: 878041). Thanks go to the Machine Learning Research Group at Oxford University and AAU colleagues: K. L. Jepsen, L. Hansen, P. Durdevic, S. Pedersen, and S. Jespersen for many valuable discussions and technical support.

## REFERENCES

- Antsaklis, P. (2000). Special issue on hybrid systems: theory and applications a brief introduction to the theory and applications of hybrid systems. *Proceedings of the IEEE*, 88(7), 879–887. doi:10.1109/JPROC.2000.871299.
- Bacci di Capaci, R. and Scali, C. (2018). Review and comparison of techniques of analysis of valve stiction: From modeling to smart diagnosis. *Chemical Engineering Research and Design*, 130, 230–265. doi:10.1016/j.cherd.2017.12.038.
- Bram, M.V., Hansen, L., Hansen, D.S., and Yang, Z. (2017). Grey-Box modeling of an offshore deoiling hydrocyclone system. *1st Annual IEEE Conference on Control Technology and Applications, CCTA 2017*, 94–98. doi:10.1109/CCTA.2017.8062446.
- Bram, M.V., Hassan, A.A., Hansen, D.S., Durdevic, P., Pedersen, S., and Yang, Z. (2015). Experimental modeling of a deoiling hydrocyclone system. In *2015 20th International Conference on Methods and Models in Automation and Robotics, MMAR 2015*, 1, 1080–1085. IEEE. doi:10.1109/MMAR.2015.7284029.
- Bram, M.V., Hansen, L., Hansen, D.S., and Yang, Z. (2018). Hydrocyclone Separation Efficiency Modeled by Flow Resistances and Droplet Trajectories. *IFAC-PapersOnLine*, 51(8), 132–137. doi:10.1016/j.ifacol.2018.06.367.
- Bram, M.V., Hansen, L., Hansen, D.S., and Yang, Z. (2019). Extended Grey-Box Modeling of Real-Time Hydrocyclone Separation Efficiency. In *2019 18th European Control Conference (ECC)*, 3625–3631. IEEE. doi:10.23919/ECC.2019.8796175.
- Bürkert Control Systems (2019). Operating Instructions, Type 8692 8693, Electropneumatic positioner and process controller. Technical report.
- Choudhury, M.A., Kariwala, V., Shah, S.L., Douke, H., Takada, H., and Thornhill, N.F. (2005). *A simple test to confirm control valve stiction*, volume 16. IFAC. doi:10.3182/20050703-6-CZ-1902.01589.
- Choudhury, M., Thornhill, N., and Shah, S. (2004). A Data-Driven Model for Valve Stiction. *IFAC Proceedings Volumes*, 37(1), 245–250. doi:10.1016/S1474-6670(17)38739-6.
- Desborough, L. and Miller, R. (2002). Increasing customer value of industrial control performance monitoring - Honeywell's experience. *AIChE Symposium Series*, 98(326), 169–189.
- Durdevic, P., Pedersen, S., and Yang, Z. (2018). Efficiency Control in Offshore De-oiling Installations. *Computers & Chemical Engineering*.
- Durdevic, P. and Yang, Z. (2018). Application of H<sub>∞</sub> robust control on a scaled offshore oil and gas de-oiling facility. *Energies*, 11(2). doi:10.3390/en11020287.
- Hansen, D.S., Jespersen, S., Bram, M.V., and Yang, Z. (2018a). Human Machine Interface Prototyping and Application for Advanced Control of Offshore Topside Separation Processes. In *IECON 2018 - 44th Annual Conference of the IEEE Industrial Electronics Society*, 2341–2347. IEEE. doi:10.1109/IECON.2018.8591309.
- Hansen, L., Durdevic, P., Jepsen, K.L., and Yang, Z. (2018b). Plant-wide Optimal Control of an Offshore De-oiling Process Using MPC Technique. *IFAC-PapersOnLine*, 51(8), 144–150. doi:10.1016/j.ifacol.2018.06.369.
- He, Q.P. and Wang, J. (2014). Valve Stiction Quantification Method Based on a Semiphysical Valve Stiction Model. *Industrial & Engineering Chemistry Research*, 53(30), 12010–12022. doi:10.1021/ie501069n.
- Jelali, M. (2006). An overview of control performance assessment technology and industrial applications. *Control Engineering Practice*, 14(5), 441–466. doi:10.1016/j.conengprac.2005.11.005.
- Jepsen, K., Bram, M., Pedersen, S., and Yang, Z. (2018). Membrane Fouling for Produced Water Treatment: A Review Study From a Process Control Perspective. *Water*, 10(7), 847. doi:10.3390/w10070847.
- Papageorgiou, D., Blanke, M., Niemann, H.H., and Richter, J.H. (2019). Robust Backlash Estimation for Industrial Drive-Train Systems—Theory and Validation. *IEEE Transactions on Control Systems Technology*, 27(5), 1847–1861. doi:10.1109/TCST.2018.2837642.
- Shoukat Choudhury, M., Thornhill, N., and Shah, S. (2005). Modelling valve stiction. *Control Engineering Practice*, 13(5), 641–658. doi:10.1016/j.conengprac.2004.05.005.